ADVANCED MATERIALS

# Supporting Information

for *Adv. Mater.*, DOI: 10.1002/adma.201703986

# Implementing Quantum Search Algorithm with Metamaterials

*Weixuan Zhang, Kaiyang Cheng, Chao Wu, Yi Wang, Hongqiang Li,* and Xiangdong Zhang**

Submitted to ADVANCED MATERIALS


# Supporting Information

**Implementing quantum search algorithm with metamaterials**

*Weixuan Zhang, Kaiyang Cheng, Chao Wu, Yi Wang, Hongqiang Li* and Xiangdong Zhang**

## *1. The protocol of implementation of Grover's search algorithm with metamaterials.*

A quantum state with uniform superposition is prepared for Grover's search algorithm. A quantum operation called Grover's iterator is then applied repeatedly to it. This operation does the following: first the amplitude of a single tagged state is inverted by using the oracle operator. The second step is an inversion of all amplitudes about their average value, which is realized by "iversion-about-average" (IAA) operation. By repeating the Grover iterator $\sim\sqrt{N}$ times, we gradually transform the state from the uniform superposition into the pure tagged state and we thus find our solution.

The Grover's search algorithm maps onto our metamaterial-based protocol as follows. The electric field amplitude of the incident microwave is recognized as the probability amplitude of the equivalent quantum state, spatial positions are used to label the items in the database, and the maximum number of the database is fixed by the full width at half maximum (FWHM) of the incident intensity profile with near-Gaussian distribution. The function of oracle block, which marks the targeted item by imprinting a spatially-dependent phase profile ($0.5\pi$ in a narrow marked area and $0\pi$ elsewhere) on the incident beam, is equivalent to the oracle operator in Grover's search algorithm. Then, a combination of two Fourier transform subblocks and the phase plate subblock can convert the phase difference marked by the oracle subblock into amplitude information by the sequences $\sim FU_0F$, which is similar to the *IAA* operation of the original quantum search algorithm. When an incident wave enters in the designed metamaterials, the profile of beam wavefront is processed iteratively as it propagates through

Submitted to

are different on the four cascaded subblocks, which results from the different values of the effective permittivities $\varepsilon_{eff}$ at different positions.

### *3. Simulation methods.*

COMSOL Multiphysics, version 5.2, is used for all simulations presented in the main text and Supplementary Information. The schematic model used in the simulation for the matamaterials (0.5-iteration) with the two-dimensional GRIN blocks and $U_{0(m)}$ blocks is shown in Figure S1. The whole metamaterial ($U_0$/*GRIN*/$U_m$/*GRIN*) presented here is limited by the width $W$ in the transverse direction $y$, and by the total length $d_0+l+d_m+l$ in the longitudinal direction $x$. Outsides the metamaterial, the metarial is defined as air (green area), and each side air region has a width of $W/4$. The left boundary of air domain is the incident port (black dash line). Extra perfectly-matched-layer regions (blue area) are used around the whole structure with thickness $\lambda_0/4$. The external boundaries are defined as scattering boundary condition. The maximum mesh size is 0.1 cm, which is fine enough for convergence.

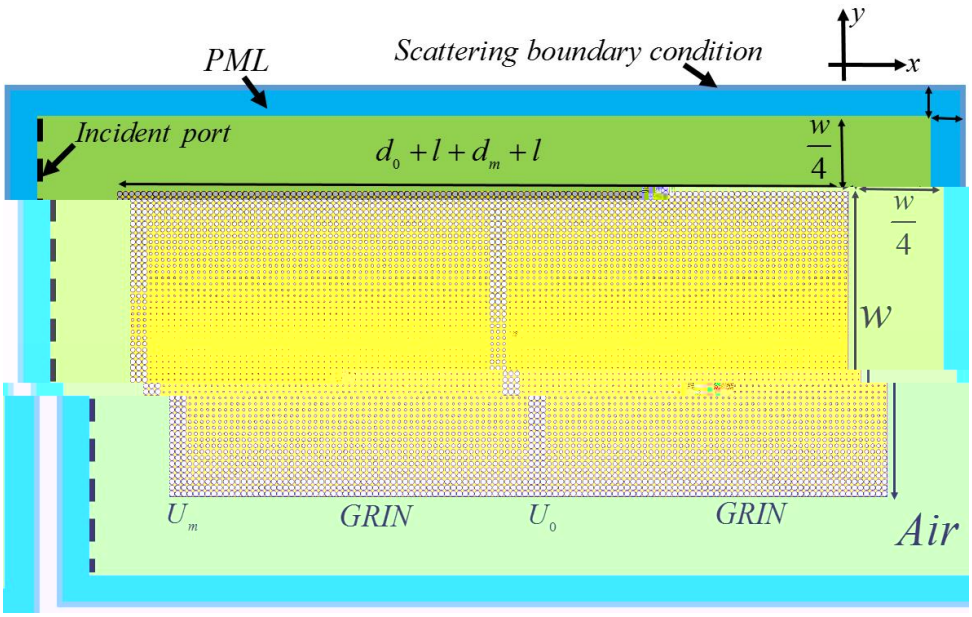


**Figure S1.** Basic model built in COMSOL.

### *4. Single-item searching with multiple iterations*

The more complicated metamaterial (compared to the case mentioned in the main text), which can simulate the searching process of a larger databases, can also be designed. Here, we present the simulation results with the marked items being found after 2.5-iterations. The parameters are chosen as: $\varepsilon_c = 8.0$, $d_m$=$d_0$=3$a$, $W$=100$a$ and $l$=120$a$, respectively. The marked items are located on the positions from $y$=-5$a$ to -2$a$. The input function is expressed as: $E(y)=exp(-y^2/50)$ with the corresponding *FWHM* value of the incident intensity equaling to $D$=10 cm. Figure S2 shows the distributions of the light intensity $|E(y)|^2$ at the output plane with 0.5 (black line), 1.0 (red line), 1.5 (blue line), 2.0 (green line), 2.5 (pink line), 3.0 (yellow line) and 3.5 (purple line) iterations, respectively. We can see that output lights are nearly all focused on the marked positions after 2.5-iterations with the total *FWHM* being d=1.19 cm. The number of iterations performed on the metamaterial is identical to the efficiency of the quantum searching arithmetic $\pi\sqrt{D/d}/4 \approx 2$.

**Figure S2.** Simulation results for the output intensity with the incident light propagating 0.5

parameters are chosen as: $\varepsilon_c = 3.0$, $d_m$=$d_0$=3$a$, $W$=153$a$ and $l$=171$a$, respectively. The marked items are located on the positions from $y$=-14$a$ to -8$a$ and $y$=8$a$ to 14$a$. The input function is expressed as: $E(y)=exp(-y^2/250)$. The corresponding *FWHM* value of the incident intensity equals to $D$=20.5 cm. Figure S3 plots the distributions of the light intensity $|E(y)|^2$ at the output plane with 0.5 (black line), 1.0 (red line), 1.5 (blue line), 2.0 (green line) and 2.5 (pink line) iterations, respectively. It is clearly shown that output lights are nearly all concentrated on the two marked positions after 2.0-iterations with the total *FWHM* being $d$=3.43 cm. In this case, the number of iterations performed on the metamaterial is consistent with the efficiency of the quantum searching arithmetic $\pi\sqrt{D/d}/4$. Consequently, we demonstrate that the designed metamaterial can also implement the multi-items searching process with quantum efficiency.

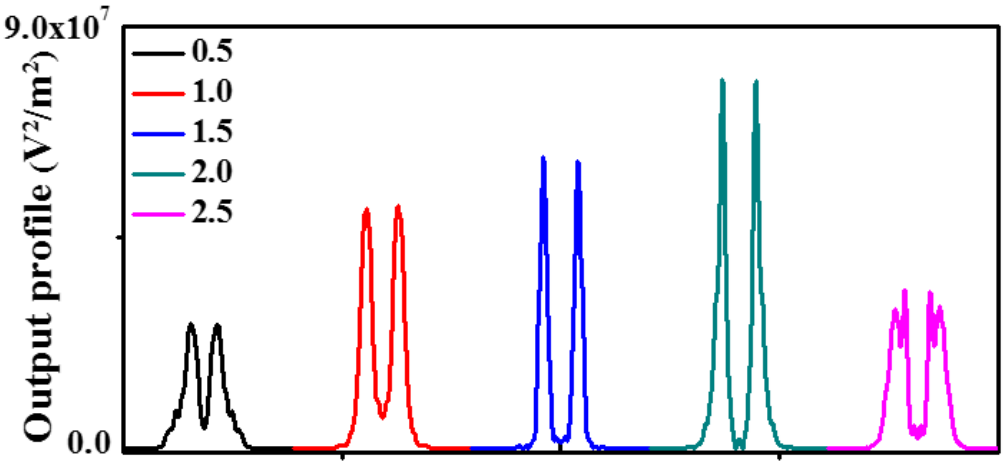


**Figure S3.** Simulation results for the output intensity with the incident light propagating 0.5 (black line), 1.0 (red line), 1.5 (blue line), 2.0 (green line) and 2.5 (pink line) roundtrips within the designed metamaterial, respectively.

### *6. Designing the ceramic ($Al_2O_3$) reflector.*

The thickness of the $Al_2O_3$ sheet has a remarkable influence on the corresponding optical response. Figure S4a shows the transmittance (black line) and reflectance (red line) as functions of the thickness of $Al_2O_3$ sheet, when the frequency of the incident light is 19.3GHz. At this

frequency, the relative permittivity of $Al_2O_3$ is 8.2. The peaks and valleys of the transmittance and reflectance repeat periodically with the variation of the thickness of the sheet. Within the machining precision, the 1 mm-thick $Al_2O_3$ sheets are chosen to be fabricated. In this condition, the multiple reflection within the $Al_2O_3$ sheet can be ignored. Figure S4b presents the transmittance and reflectance as functions of the incident light frequency, when the thickness of the $Al_2O_3$ sheet is 1 mm. We can see that changes of the transmittance and reflectance are negligible in the bandwidth of the incident pulses**.**

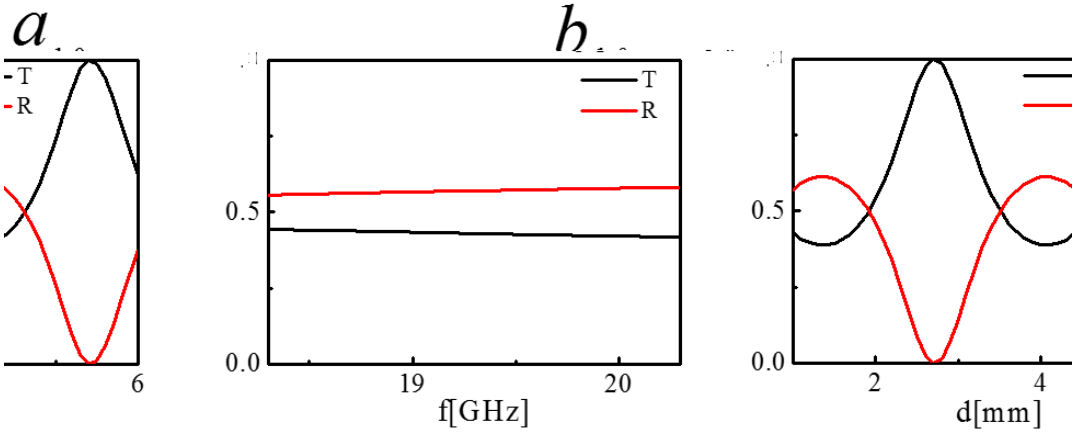


**Figure S4.** a) The relationship between the thickness and transmittance (reflectance) of the ceramic sheet with the incident frequency being 19.3GHz. b) The relationship between the incident frequency and transmittance (reflectance) with the thickness of the ceramic sheet being 1 mm.

**References**

[S1] P. Halevi, A. A. Krokhin, J. Arriaga, *Phys. Rev. Lett.* **1999**, 82, 719-722.
[S2] B. Vasić and R. Gajić, *J. Appl. Phys.* **2011**, 110, 053103-053108.